ISSN 2635-1676, Nanobiotechnology Reports, 2023, Vol. 18, No. 6, pp. 829–841. © The Author(s), 2023. This article is an open access publication.
Russian Text © The Author(s), 2023, published in Rossiiskie Nanotekhnologii, 2023, Vol. 18, No. 6, pp. 723–736.

REVIEWS

Structural Transformations and Formation of Microstructures and Nanostructures in Thin Films of Chalcogenide Vitreous Semiconductors

S. V. Zabotnov[a,*], P. K. Kashkarov[a,b,], A. V. Kolobov[c,***], and S. A. Kozyukhin[d,****]**

[a] *Faculty of Physics, Lomonosov Moscow State University, Moscow, 119991 Russia*
[b] *National Research Center "Kurchatov Institute," Moscow, 123182 Russia*
[c] *Herzen Russian State Pedagogical University, Institute of Physics, St. Petersburg, 191186 Russia*
[d] *Kurnakov Institute of General and Inorganic Chemistry, Russian Academy of Sciences, Moscow, 119991 Russia*
**e-mail: zabotnov@physics.msu.ru*
***e-mail: Kashkarov_PK@nrcki.ru*
****e-mail: akolobov@herzen.spb.ru*
*****e-mail: sergkoz@igic.ras.ru*

Received July 7, 2023; revised July 7, 2023; accepted July 25, 2023

Abstract—Chalcogenide vitreous semiconductors (ChVSs) are of both fundamental and applied interest as materials in which reversible structural transformations within the amorphous phase and phase transitions to the crystalline state can be effectively implemented and various microstructures and nanostructures can be obtained as a result of external effects. One of the most promising methods for such ChVS modifications is the pulsed-laser-irradiation technique, which is a noncontact technology of local impact and makes it possible to change the structural, optical, and electrical properties of samples in a wide range. This includes methods based on the precision formation of a surface microrelief and nanorelief, and high contrast in the conductivity and refractive index between the crystalline and amorphous phases. This work reviews key publications on the structural modification of thin films from the most widely studied binary and ternary ChVS compounds (As_2S_3, As_2Se_3, $Ge_2Sb_2Te_5$, etc.) to show the use of irradiated samples as metasurfaces for photonic applications and promising phase-change data storage.

DOI: 10.1134/S2635167623600542

TABLE OF CONTENTS

INTRODUCTION

The modern world cannot be imagined without a huge number of electronic devices, such as computers, mobile devices, the Internet of things, and other devices. The functioning of the vast majority of them is based on semiconductors. The modern semiconductor industry is based mainly on the use of silicon technology and III–V compounds. At the same time, there are other classes of functional semiconductor materials, among which, chalcogenide semiconductors (compounds based on sulfur, selenium, and tellurium) occupy a special place. These materials are of interest since they have exhibited the vast majority of semiconductor effects significant for the development of science.

In 1833, Faraday for the first time observed an increase in conductivity with temperature increase (a typical semiconductor dependence) on silver sulfide [1]. Forty years later, Smith discovered the phenomenon of photoconductivity while working with selenium [2] and Brown discovered the rectification effect at the contact between metal and lead sulfide [3]. The photovoltaic effect was also observed in selenium for the first time [4].

Studies of chalcogenide semiconductors continued; special interest in them flared up with renewed vigor in 1955 after the discovery of the semiconductor properties of chalcogenide glasses with complex composition by Goryunova and Kolomiets [5]. As emphasized by Mott in his Nobel lecture [6], this discovery

changed the existing paradigm about the nature of the band gap in noncrystalline semiconductors. Before the Kolomiets–Goryunova discovery, the band gap was believed to be generated exclusively due to the long-range order existing in crystals.

The next significant impetus for research into vitreous (amorphous) semiconductors was provided by the studies of Kolomiets and Lebedev: in 1963, they discovered the switching effect in chalcogenide glasses with a sawtooth voltage applied to them [7]. A few years later, Ovshinskii showed that thin films of amorphous chalcogenides after switching were characterized by transformation of the local structure and the low-resistance state was maintained even after voltage removal; i.e., a memory effect is observed [8]. These effects found application in rewritable optical disks (from CDs and DVDs to Blu-Ray disks) and in the latest implementation of nonvolatile 3D-XPoint memory, produced jointly by Intel and Micron under the Optane brand [9, 10]. It should be noted that both the memory elements themselves and selectors were made of amorphous chalcogenides in Optane solid-state memory [11].

Among other studies over recent years, one should note a great interest in a class of materials such as topological insulators. The vast majority of topological insulators are produced based on binary chalcogenides (Sb_2Te_3, Bi_2Te_3, and Bi_2Se_3) [12, 13], as well as CdTe–HgTe structures. The publication [14] in 2007 is generally considered the first study that experimentally demonstrated the properties of a topological insulator in CdTe–HgTe structures. In this regard, it should be noted that the existence of two-dimensional edge states protected by symmetry with respect to time reversal (i.e., topological states) was theoretically predicted 20 years earlier by a team of Soviet physicists Pankratov, Pakhomov, and Volkov [15].

Chalcogenide compounds are also typical representatives of the currently actively studied class of two-dimensional semiconductors. These primarily include transition-metal dichalcogenides [16], as well such a material as InSe, which has a record carrier mobility [17]. Taking into account the diversity of electrophysical and optical effects and application possibilities, the history of chalcogenide semiconductors is far from being limited by these events.

In this review, we focus on the property of amorphous chalcogenides (also called chalcogenide vitreous semiconductors (ChVSs)), such as the ability to reversibly change their structure and properties, including nanostructuring and microstructuring, under external effects, in particular, light effects. Let us consider the prospects for creating photonic and phase-memory devices based on thin films of these materials.

1. PHOTOINDUCED EFFECTS IN ChVSs

A photoinduced change in the properties of ChVSs was first demonstrated in [18], where it was shown that the irradiation of As_2S_3 films with light led to a reversible change in their transmittance, so-called reversible photodarkening. The photodarkening is accompanied by a change in film thickness [19, 20], which can be used for the production of lenses and diffraction gratings. The photodarkening-induced change in the rate of ChVS dissolution in different etchants makes them promising materials for use as photoresists [21]; in addition, the use of synchrotron radiation makes it possible to form structures about 30 nm in size in ChVSs [22]. X-ray scattering experiments showed that all these processes were determined by reversible changes in the short-range order of ChVSs [23].

In the case of linearly polarized light, photoinduced anisotropy is oriented to ChVSs; it can be reoriented or erased by further irradiation with orthogonally polarized or unpolarized light, respectively [24]. Irradiation with polarized radiation leads to anisotropic mass transfer of the film substance [25].

It is important to note the process of reversible crystallization–amorphization. Thus, an $As_{50}Se_{50}$ film thermally crystallized into the realgar structure returns to the amorphous state as a result of further illumination [26].

A particular place among ChVSs, which exhibit reversible phase transitions ("amorphous phase–crystalline phase–amorphous phase") and are called phase-change materials (PCMs), is occupied by tellurium-based alloys. As noted above, these materials have found wide application in optical and electrical memory cells [27].

Most photoinduced effects obey the law of reciprocity (when the resulting effect is proportional to the radiation dose, i.e., the product of the intensity of light exposure to its time). Of particular interest are processes under the effect of ultrashort (femtosecond) laser pulses when intense electronic excitation exceeds thermal processes with respect to the rate and efficiency of structural transformations [28–32].

Phase transitions between two states and associated structural transformations are responsible for the possibility of data recording and rewriting in ChVSs. The compactness and speed of information encoding by focused laser radiation make it promising to use thin films based on PCMs, primarily the $Ge_2Sb_2Te_5$ compound (GST225) with a high contrast of the refractive index between the crystalline and amorphous phases [33], as data carriers, which have competitive advantages over existing flash and DRAM memory technologies [34]. In addition, structured thin ChVS films are of undoubted interest for photonics as metasurfaces [35–37] and waveguide structures [38, 39], which are transparent in the telecommunication range. In these cases, structuring can consist not only in laser-

induced phase transitions (which, in particular, lead to nanocrystallization of the material), but also result from so-called direct laser recording of a micron and submicron relief on the irradiated surface. Therefore, the interest of researchers in the field of the laser structuring of ChVSs is determined both by the possibility of controlling the phase state of the material, including its reversible processes, and by technologies for a direct change of the surface morphology by irradiation with laser pulses with certain energy and time parameters along predefined trajectories of the beam relative to the sample.

Therefore, further progress in the creation of devices and systems based on ChVSs for applications should be determined by the extent to which researchers will understand the fundamental nature of crystallization and reamorphization in these materials, as well as the pattern of relief modification under laser irradiation or other external (thermal and electrical) effects and, accordingly, the ways to control these processes.

2. CRYSTALLIZATION AND NUCLEATION IN ChVSs AND PHASE-CHANGE MATERIALS

The crystallization of PCMs such as ChVSs is described based mainly on three approaches: the classical crystallization model, the Johnson—Mehl—Avrami—Kolmogorov (JMAK) theory, and the nonisothermal crystallization model. Let us consider the features of these approaches.

The crystallization of liquids or deposition of crystals from solutions are described using a model based on the consideration of the process of nucleation and the associated process of crystal growth. The approach was proposed by Tammann about 100 years ago [40–42] and has undergone numerous experimental tests at different facilities over time. Despite the somewhat simplified model representations, the approach is quite applicable to real systems. The essence of the approach is that the crystallization process can be described as the sum of two processes, namely, as steady-state nucleation (this is the number of crystalline centers capable of growth, which are formed per unit volume per unit time in supercooled melt as a result of thermal fluctuations) and as crystal growth, the mechanisms of which can be different. For instance, the standard model assumes that all positions are equivalent on the nucleus surface and each of them can serve as a site for further crystal growth. Models of the growth of two-dimensional nuclei are also considered; these models are based on the addition of a particle (molecule), e.g., to the face of a screw dislocation.

In the general case, the driving force of the crystallization process is determined by the difference between the free energies of the melt and crystal, which is generated in the supercooling region of the liquid phase, i.e., at temperatures below the melting point; the second feature of the process is that crystallization begins after a certain time delay. This classical approach to the phenomenon of crystallization is quite well described by mathematical expressions, experimentally confirmed for different systems, and described in many monographs and articles, e.g., in [43, 44].

Numerous studies have shown that the maximum crystallization rate under conditions of homogeneous steady-state nucleation in inorganic glass-forming systems (including ChVSs) is achieved under conditions of moderate melt supercooling, since the nucleation rate under strong supercooling conditions is low due to the high viscosity of the melt, while this indicator is insignificant at low supercooling as a result of the great value of the free energy of nucleation [45, 46]. We note that the description of real crystallization processes, e.g., under the effect of laser radiation, should take into account that this process occurs with a time delay, i.e., it is nonsteady state, at least in the initial time period. Therefore, the kinetic factor is an important parameter during the study of the pulsed-laser crystallization of thin-film noncrystalline semiconductors. It is also necessary to take into account that, in the general case, homogeneous nucleation may be additionally "superimposed" with heterogeneous nucleation, which, in turn, is determined by the presence of interfaces between the corresponding phases, foreign inclusions, and other inhomogeneities in the material. Therefore, it can be stated that the maximum rate of crystallization will be observed under the condition of maximum overlap of the curves characterizing the rates of nucleation and crystal growth.

An approach called the JMAK theory is often used to describe the isothermal crystallization of ChVSs and PCM materials; this approach makes it possible to calculate the volume percent of the crystalline fraction without knowing certain nuances associated with the nucleation rate and crystal growth in the amorphous matrix [47–49].

The JMAK equation has a relatively simple analytical form

$$x(t) = 1 - \exp[-kt^n], \quad (1)$$

where t is time, n is the Avrami coefficient, and k is the effective constant of the rate of the crystallization process. Accordingly, if we experimentally measure the percent of the crystalline fraction x at different time intervals, the slope of the straight line in the coordinate system $\ln[-\ln(1-x)] = f(\ln(t))$ will give the value of the Avrami coefficient and the intersection with the coordinate axis will give the value of the rate constant. Theoretically, the Avrami coefficient n included in Eq. (1) makes it possible to estimate the size of the growing crystals in a number of cases: the number of spherical crystals grows at $n = 3$, while flat structures are formed at $n = 2$. The effective rate constant k integrally takes into account both the nucleation rate and

crystal growth rate and its temperature dependence obeys the classical Arrhenius law, according to which the activation energy value corresponds to the crystallization activation energy (E_a), without dividing the process into nucleation and particle growth, and the pre-exponential factor, or frequency factor (ν), is a formal value without a clear physical meaning, somehow characterizing the crystallization of a certain phase. Therefore, parameters n, ν, and E_a can effectively characterize the crystallization process within the JMAK formalism during the performance of a simple experiment on isothermal annealing of the test material.

Numerous studies of ChVSs and PCM materials using the JMAK model [50–53] have shown that the above key characteristics describing crystallization can vary in a fairly wide range even for formally the same chemical composition. For instance, the crystallization activation energy can vary from 0.81 to 3 eV for the most studied PCM GST225 material, although most of the published values range from 2.2 to 2.6 eV [54]. A similar situation is observed with the Avrami coefficient: its spread is 2.5 to 5.8; the frequency factor has an even greater range: from 10^{17} to 10^{86} s^{-1}. These striking differences are obviously determined by the fact that the JMAK model is built on a number of assumptions that are not implemented in ChVSs to the required extent; specifically, the process of nucleation is uniform throughout the volume and steady state; the rate of crystal growth does not depend on the size of the nucleus and is controlled by its surface. Such assumptions do not work in many cases, in particular, under conditions of nonsteady-state and nonisothermal processes, which are most important for PCMs during the operation of real devices, such as memory cells. We note that attempts were made to improve the JMAK model, taking into account nonuniform nucleation, anisotropic crystal growth, nonisothermal heating, etc. [55, 56].

As applied to amorphous thin films and ChVS and PCM films and their crystallization under the influence of pulsed-laser radiation, including a femtosecond laser, the classical approach gives a fairly good agreement with the experiment in some cases. For instance, the work [57] described the process of crystallization of an amorphous GST225 film under the effect of a single laser pulse, (τ = 185 fs, λ = 1030 nm) within the solution of a system of equations describing the temperature dependences of the time of crystallite nucleation and the rate of nucleation and growth of crystallites. This made it possible to construct so-called TTT diagrams (time-temperature-transformation diagrams) and determine the critical rate of crystallization, when the minimum detectable limit of the crystalline phase, equal to 10^{-8} of the volume fraction, and the cooling rate required for complete crystallization of the amorphous matrix are generated. In the described approach, the laser pulse is considered as a point source of heat for the film, which made it possible to accurately describe the distribution of the crystalline phase in the amorphous matrix at different pulse energy levels; the distribution calculated in this case was well consistent with the experiment. An important assumption in this approach to the crystallization process is the consideration of kinetic processes; namely, it is assumed that crystallization should have a shorter characteristic time than that of thermal diffusion. In other words, crystallization should end before the heat reaches the substrate. Otherwise, a single pulse is insufficient to crystallize the GST225 film.

An important factor during the phase transition of PCMs is consideration of the pattern of the external effect, i.e., the answer to the question whether the source of the external effect serves solely as a source of heat or its electromagnetic nature should be also taken into account (here, the matter concerns only an electric field or a light wave). In [58, 59], a crystallization model is proposed for amorphous GST225 films under the effect of a strong electric field. The model was based on the earlier ideas of S. Ovshinskii that, firstly, nucleation in ChVSs depends on the electric field, which leads to a decrease in the activation energy of nucleation when the field is applied; secondly, under conditions of strong fields corresponding to switching (actually phase transition), crystalline nuclei are generated in the form of filaments or elongated threads and the amorphous high-resistivity phase can be shunted. This model showed that the crystalline phase could grow at the end of the filament at a significant rate as a result of the concentration of the electric field and a significant decrease in the energy barrier to nucleation in this region. It is interesting that the model is also applicable for weakly absorbing laser exposure (i.e., exposure excluding material heating), since the electric field of the laser promotes the growth of crystals along the direction of the polarization vector of the electric field.

3. ChVS METASURFACES

Since a significant amount of studies of ChVSs is devoted to thin microstructured and nanostructured films based on ChVSs, we can distinguish the use of such systems as metamaterials and metasurfaces.

Metamaterials, which have attracted keen interest from researchers over the past few decades (although they became known much earlier), are usually a composite with properties determined by an artificially created periodic structure with electromagnetic properties that are not observed in nature. For instance, well-known photonic crystals exhibit a periodic change in the refractive index in spatial directions, with a period comparable to the wavelength of light. Without going into details of the physics of metamaterials, we can recommend the latest reviews on this topic [60–62].

Metasurfaces are a two-dimensional counterpart to metamaterials; they are well suited for controlling light, since they tend to have lower losses than bulk metama-

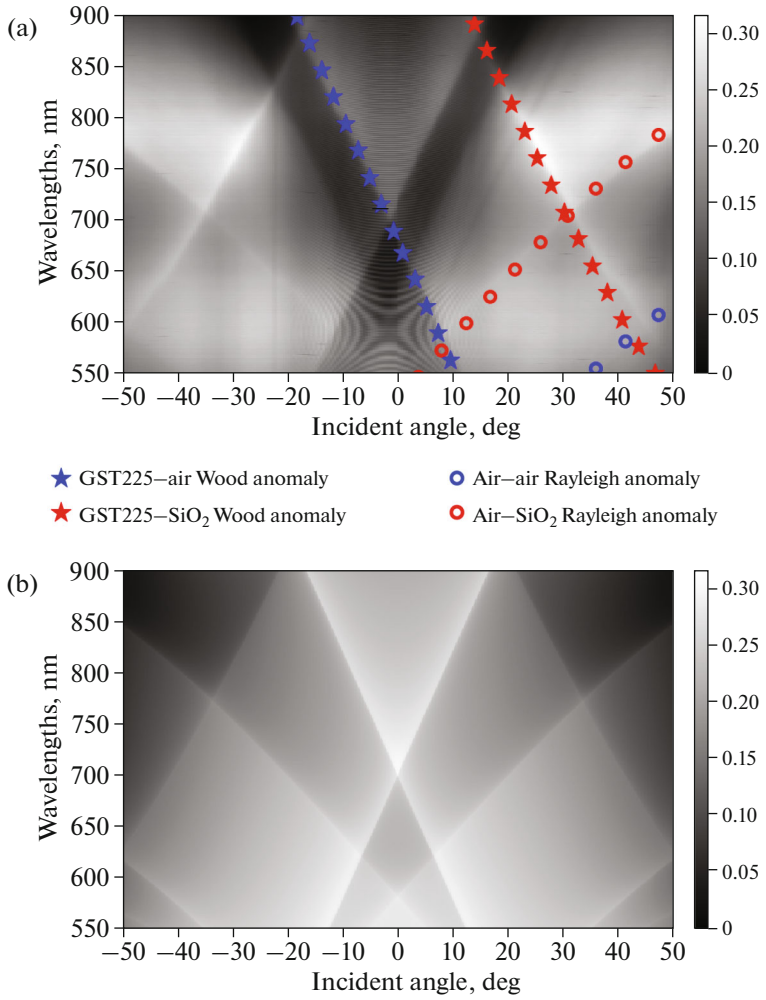

Fig. 1. Experimental (a) and theoretical (b) angle-resolved reflection spectra for a GST225 thin-film surface grating in the amorphous phase on a quartz substrate. The term *air–air Rayleigh anomaly* refers to the diffraction of a plane wave into the surrounding medium (air). The term *air–SiO_2 Rayleigh anomaly* means the diffraction of a plane wave from air into the quartz substrate. The same terminology is used for Wood's anomaly [63].

terials and their production is generally simpler (they are sometimes termed as *metafilms*). Metasurfaces randomly change the front and phase of light incident on them. Typically, lenses are used to change the light front. Their use makes it possible to control the light front; however, this control most often takes up a large amount of space and, accordingly, weighs a lot. Therefore, the replacement of lenses by metasurfaces is a technically attractive idea, and an almost unlimited number of devices can be created based on metasurfaces. The dimensions of all currently existing optical systems (filters, detectors, and irradiators) can be significantly reduced through the use of metasurfaces.

Tunable (reconfigurable) metasurfaces formed using ChVSs as a functional material have new prospects for development and further commercialization. We note that such nanostructures are also interesting from the point of view of fundamental physics. For instance, the work [63] shows that quasi-waveguide modes can be effectively excited in surface gratings based on the GST225 chalcogenide semiconductor, which, in turn, leads to the appearance of narrow resonances (Rayleigh and Wood anomalies) in the optical response of the structures at certain values of frequencies and wave vectors. The experimental dependences of the observed peaks in the angle-resolved reflectance spectra, obtained by spectral Fourier microscopy are well consistent with the theoretical calculations (Fig. 1).

On the whole, metasurfaces based on films of phase-change memory materials, such as GST225, are promising for optical modulation [35], in particular, for controlling the beam shape and the direction of propagation of the light beam [64], as well as for controlling the absorption of optical systems; the 7 : 1 optical contrast is reached during the phase transition from the amorphous to the completely crystalline phase [36]. Such metasurfaces are of interest for polarization conversion [37]; in addition, they can be used

to create diffractive optical elements of rewritable holograms (so-called computer-generated holograms (CGHs)) [65] and potentially energy-independent color displays, in which the GeTe-type ChVS crystalline phase coated with periodically placed aluminum circles selectively absorbs RGB light, depending on the circle diameter, and, accordingly, generates pixels of different colors, and the amorphous phase suppressing the resonant absorption of light exhibits pseudo-white reflectivity [66]. The change in the degree of crystallinity in a metafilm based on GST225 using a pulsed laser [67] showed the possibility of creating tunable narrow-band filters in the mid-IR wavelength range of 3–5 μm.

Until recently, the main problems in the development and commercialization of these metasurfaces were the process of initiating a change in the phase state and, consequently, the creation of reconfigurable metasurfaces, as well as a high level of optical losses in these metasurfaces. Phase transformations in the functional material of metasurfaces are initiated using two main approaches, laser radiation or passing electric current through a PCM, which, accordingly, requires the use of a large laser system or many additional technological processes providing the local heating of nanoscale areas of the metasurface.

An example of solution to this problem is the possibility of using an approach proposed in [68], where an external microheater controlled by electrical pulses with various shapes and durations was used to switch metasurface elements based on GST225 (Fig. 2).

The problem of optical losses can be solved by changing the composition of functional PCMs to achieve maximum transparency of the amorphous state while maintaining sufficient optical contrast in the wavelength range required for operation of the device under development. For example, binary Sb_2S_3 and Sb_2Se_3 ChVSs, which have a high transparency in the telecommunication range of about 1550 nm and a refractive index well consistent with the components of silicon photonics, are promising from this point of view [69]. However, changes in the refractive index are significantly lower during the phase transition for these binary compositions than for GST, which, accordingly, requires a larger (by about 3 times) optical path to obtain the same phase shift at the same material thickness.

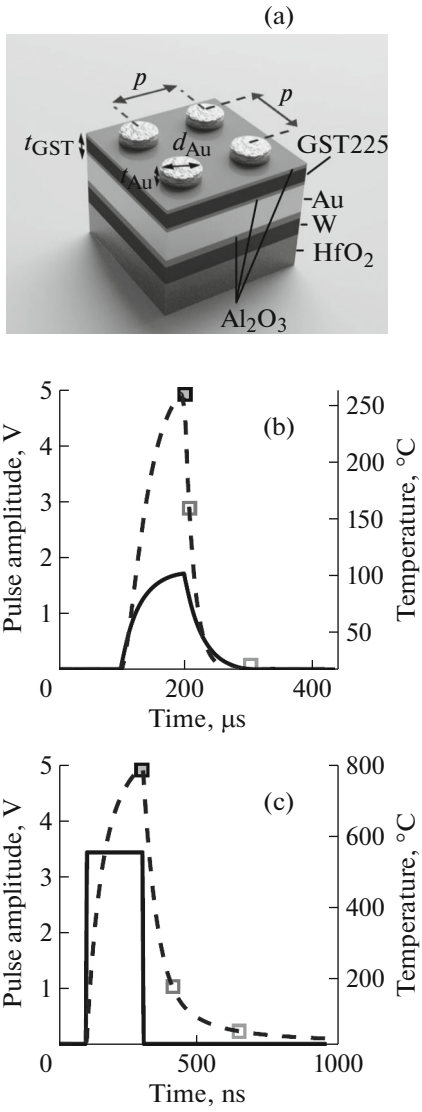

Fig. 2. Schematic representation of a metasurface (a) and kinetics of its heating when electrical pulses are applied to the heater for complete crystallization (b) and amorphization (c) of the GST225 layer. Solid lines indicate the envelopes of the electrical signal supplied to the microheater and the dotted lines show heating kinetics [68].

4. LASER-INDUCED PERIODIC SURFACE STRUCTURES AND ARTIFICIAL ANISOTROPY IN THIN ChVS FILMS

Irradiation with ultrashort laser pulses with a duration of no more than a few units of picoseconds causes not only relatively quick photoinduced phase transitions in thin ChVS films, but also (under certain conditions) the formation of surface gratings with periods that are close to the wavelength of the structuring laser pulses [70, 71] or even several times smaller than their wavelength [72, 73].

As a rule, the formation of such laser-induced periodic surface structures (LIPSSs) is determined by the excitation of surface plasmon polaritons by femtosecond laser pulses [71, 73]. A surface electromagnetic wave photoinduced in this way can interfere with the incident radiation and lead to the appearance of a resulting standing wave, which induces both the periodic modulation of phase transitions in the surface layer and (if the ablation threshold is exceeded) the formation of a periodic relief on the micron and submicron scales. In this case, the irradiated surface

should not be necessarily a metal for the generation of plasmon polaritons: the sufficient concentration of free charge carriers during the process of LIPSS formation is provided by the generation of free charge carriers in the field of high-power femtosecond laser pulses [74].

The theory of LIPSS formation began to be actively developed in the early 1980s by the group of Professor Sipe [75], as well as by Emel'yanov et al. [76, 77] and other scientists. It was shown that the period and orientation (perpendicular or parallel to the polarization of the structuring laser pulses) of appearing structures depended on the values of the complex dielectric constants of the environment and the surface layer during irradiation. In turn, according to the Drude theory, the latter value directly depends on the value of the laser-pulse energy fluence absorbed by the surface, which was reflected in [71, 78], where it is shown that the energy characteristics of incident laser pulses are correlated with the period and the orientation of appearing LIPSSs through the concentration of free-charge carriers and the value of the complex dielectric constant of the surface layer during irradiation.

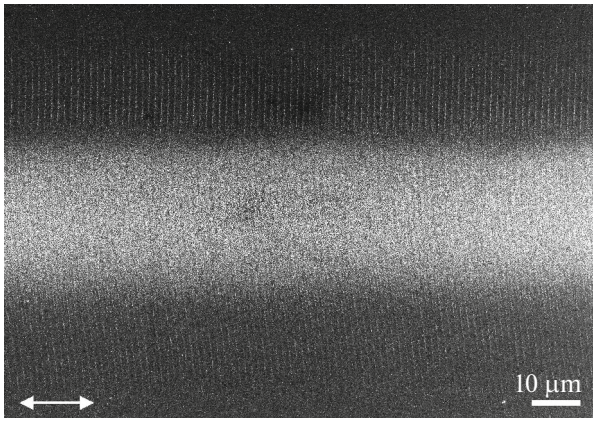

Fig. 3. Scanning electron microscope (SEM) microphotograph (130 nm thick) of a GST225 film on a thermally oxidized silicon substrate irradiated with 750 laser pulses (135 fs, 1250 nm, 0.1 J/cm^2). The light horizontal band corresponds to the reamorphized region along the path of the irradiating laser beam with a Gaussian profile in its central part. The direction of the electric-field strength is indicated by an arrow [71].

Despite the advances achieved through the development of femtosecond-laser technology in the formation of LIPSSs on different surfaces of metals, semiconductors, and dielectrics, the interest of scientists in such structures has been stimulated by challenges of finding ways to miniaturize memory elements in the last decade. In particular, the classical recording of information by a focused beam of light is spatially limited by the diffraction limit, $\lambda/2n$, where λ is the light wavelength and n is the refractive index of the medium carrying the information. The decrease in the λ value and work with UV radiation involve significant difficulties in information encoding and decoding and makes these related technologies much more expensive than technologies used in the variant with visible or near-infrared radiation. At the same time, the creation of regions with periodic modulation of the relief on wavelength and subwavelength scales using laser radiation makes it possible to increase the volume of information encoded in one memory cell (voxel) without reducing the wavelength of the structuring radiation as a result of artificial anisotropy [79–81], which is determined by mechanical stresses in the selected direction or by periodic modulation of the dielectric constant [82]. In this way, the direction of the anisotropy axis and value of birefringence and dichroism, which is determined by the polarization and energy fluence of the structuring laser pulses, respectively, currently make it possible to encode up to 8 bits of information (instead of 1 bit) in a voxel of fixed volume without reducing the wavelength [83].

However, the above-listed works describe experiments either with thin films of amorphous silicon, in which LIPSSs and regions appear in the nanocrystalline phase after irradiation, or with sodium borosilicate and quartz glasses. In the former case, the practical use of these materials as a basis for information carriers is significantly limited by the relatively low contrast of optical properties of amorphous and crystalline silicon; in the latter case, it is highly limited by the impossibility of rewriting information. The use of ChVSs makes it possible to largely avoid these limitations and simultaneously allow the formation of anisotropic regions with LIPSSs, which has been demonstrated in studies with thin films of GST225 over the past 5 years.

Thus, the change in the type of substrates on which thin films are applied [71, 84] and regulation of the energy, number, and wavelength of laser pulses [72, 85] make it possible to control the LIPSS morphology: gratings can be oriented parallel or perpendicular to the polarization and their period is approximately equal to or several times lower than the wavelength of incident radiation λ. The typical image of LIPSSs on a thin GST225 film is shown in Fig. 3.

It is important to note that the appropriate parameters of pulse irradiation in the transparency region of GST225 with λ from 800 to 2000 nm make it possible to produce LIPSSs with clearly defined subwavelength periods Λ obeying the law $\Lambda = \lambda/2n$ [72], where the values of the refractive index are $n \approx 4$ in the given spectral range for amorphous GST225 [33], and provide periodic modulation on the nanoscale.

At the same time, reversible "amorphous–crystalline" GST225 phase transitions and the formation of different types of LIPSSs by varying the energy inside the laser beam, polarization, and wavelength of laser pulses make it possible to carry out rewriting of the surface gratings and information encoded in these gratings [71, 72] (Fig. 3).

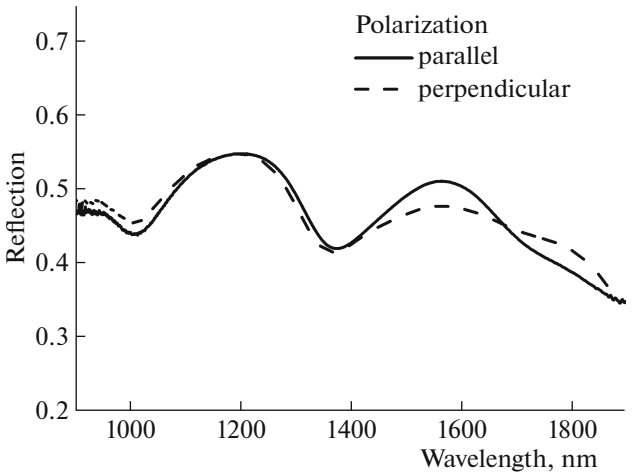

Fig. 4. Reflection spectra of a 200-nm-thick GST225 film on a thermally oxidized silicon substrate irradiated with 240 laser pulses (135 fs, 1250 nm, 0.2 J/cm^2). The direction of polarization of light incident at an angle of 13° to the normal line is compared with the scanning direction of the surface-modifying laser beam. The orientation of the LIPSS is orthogonal to the scanning direction [87].

The periodic alternation of regions in the amorphous and crystalline phases inside the formed LIPSSs [72, 85, 86] (so-called phase-change gratings) determine a clearly defined the form anisotropy [82] in the studied structures based on GST225 and, consequently, the anisotropy of their optical and electrical properties. An attempt at a comprehensive analysis of this topic was carried out in [87]. The measured reflection spectra in the near-IR range show that the values of the reflection coefficients can differ by up to 4%, depending on the polarization of the incident light in the presence of LIPSSs in the irradiated film (Fig. 4), and the behavior of these spectral dependences is in good agreement with the simulation results within the generalized Bruggeman model for LIPSS-simulating nanocomposite laminar media [88, 89].

The anisotropy of the conductivity of GST225 films that were considered in the same work is much more pronounced and can reach 5 orders of magnitude for measurements in the temperature range of 200–400 K at a direct current applied in two mutually orthogonal directions in the sample plane. This significant contrast is explained by the periodic alternation of GST225 regions in the form of parallel lines in the crystalline and amorphous phases, when the conductivity proves to be maximum with current applied along the lines as a result of the effective transfer of charge carriers through crystalline channels and the amorphous regions act as barriers in the orthogonal direction.

As a result, along with reversible phase transitions, the existence of LIPSSs in GST225 films irradiated with femtosecond laser pulses opens up new horizons for the use of these structures with artificial optical and electrophysical anisotropy as rewritable memory elements sensitive to the polarization of incident light and current applied in the film plane.

Such LIPSSs, when produced with high quality using femtosecond laser pulses, also demonstrate the properties of the diffraction grating. Thus, the work [90] experimentally demonstrated the possibility of recording two-dimensional structures (with linear dimensions of 1 mm in length and about 50 μm in width) on amorphous GST225 films during irradiation with femtosecond pulses; they consisted of 50 parallel high-quality alternating amorphous ridges and crystalline cavities. The period of such structures corresponded to the irradiation wavelength and the relief height was only 8 nm, which suggests the formation of an almost two-dimensional structure. This type of region was actually a two-phase binary periodic structure, which can be used as a diffraction grating. The study experimentally demonstrated the formation of a diffraction pattern upon the reflection of light and determined the efficiency of diffraction orders for the TM and TE modes, when incident waves are charcterized by an electric-field-strength vector lying in the plane of light incidence and orthogonally to it, respectively. It was concluded that the relative intensity of diffraction orders could be used to determine the topography of the formed LIPSSs and that this approach allowed for direct optical control of the laser writing process in situ.

Various types of surface structures can also be formed in arsenic sulfide (As_2S_3) films: surface one-dimensional gratings, ring-shaped concentric structures, and nanopillars [73] (Fig. 5). The formation of a certain type of structures and their period and orientation are determined by the number and energy density of laser pulses acting on the material.

Based on the results of the analysis of reflection from the irradiated surface using the “pump–probe” method, the following scenario for the evolution of the appearing structures was proposed in [73]. During irradiation by several pulses, the interference of excited plasmon polaritons with incident radiation leads to the formation of surface gratings with a period close to the wavelength of the structuring radiation (800 nm) and an orientation perpendicular to its polarization (Fig. 5a). An increase in the number of pulses (starting from 10) leads to additional redistribution of the electromagnetic field of incident radiation on the formed relief, thereby additionally leading to the formation of LIPSSs oriented along the polarization with a period of about 200 nm (Fig. 5b) and nanopillars (Fig. 5c). A further increase in the number of pulses to 50 also leads to the formation of concentric rings with a period of about 700 nm, which result from incident radiation reflected from the surface of the formed crater (Fig. 5d).

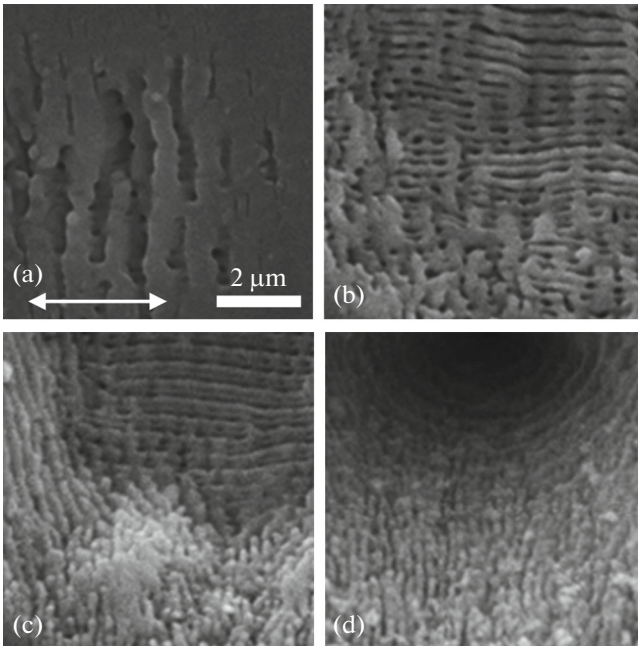

Fig. 5. SEM images of an As_2S_3 film irradiated with 2 (a), 10 (b), 20 (c), and 50 (d) laser pulses with a wavelength of 800 nm and an energy of 6.2 mJ/cm^2. The direction of the electric-field strength is indicated by an arrow [73].

We recently obtained similar LIPSSs in thin films of arsenic selenide (As_2Se_3) as a result of their structuring by radiation at the second optical harmonic frequency from a Satsuma femtosecond laser (Amplitude Systems) (515 nm, 300 fs, 0.1 μJ). Irradiation with 200–800 laser pulses leads to the formation of LIPSSs with a period of about 180 nm, which are oriented parallel to the polarization of the structuring radiation (Figs. 6a and 6b). The increase in the number of pulses in the center of the crater involves the formation of additional orthogonal gratings with an average period of 460 nm (Fig. 6c).

The simultaneous existence of several types of LIPSSs in the same crater is most likely determined by the inhomogeneous intensity distribution along the profile of the Gaussian laser beam used for irradiation. Different intensities lead to an uneven spatial distribution of the concentration of photoinduced charge carriers in the surface region, which, in turn, determines the variation in the values of the complex dielectric constant and conditions for the excitation of surface-plasmon polaritons, which are responsible for the formation of the subwavelength surface relief [71, 74, 78].

We note that the above-listed structures simultaneously coexist within the ablation crater; i.e., so-called hierarchical structures are formed, which significantly expands the possibilities of designing metasurfaces based on thin As_2S_3 films.

In addition to the classical plasmon-polariton mechanism of LIPSS formation, it is also technologi-

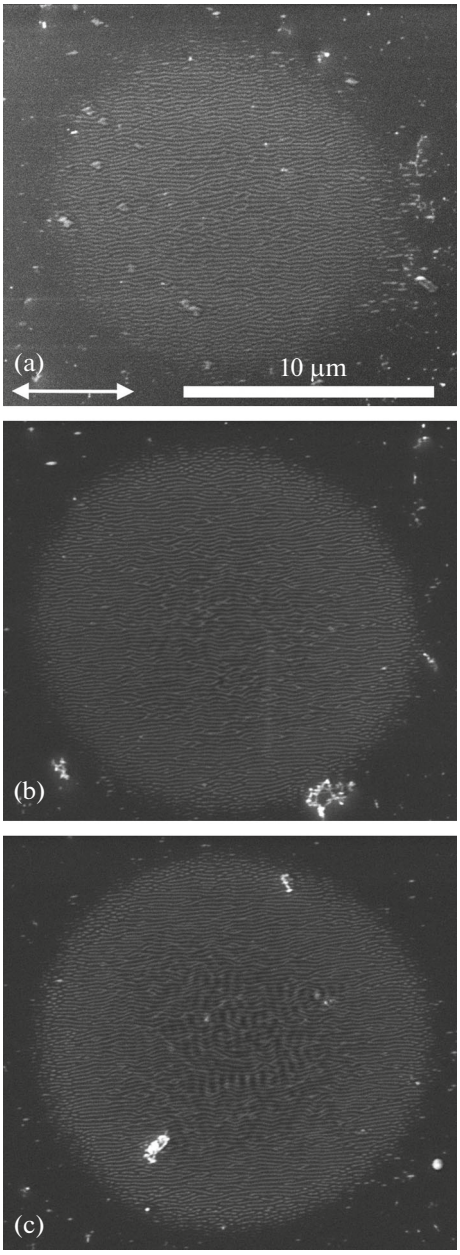

Fig. 6. SEM images of an As_2Se_3 film with a thickness of 840 nm on a substrate with a conductive sublayer ($Cr/SiO_2/Si$), irradiated with 200 (a), 800 (b), and 1200 (c) laser pulses. The direction of the electric-field strength is indicated by an arrow.

cally possible to implement other approaches to significantly reduce their periods. Thus, the work [91] describes experiments to reduce the period of the formed LIPSSs in As_2S_3 films by 2 times via rotation of the sample by 90° at the second stage of its irradiation in the raster scanning mode with a laser beam, which, according to calculations, leads to resonant localization of the electromagnetic field along the ridges of the grating formed as a result of the first scanning and to

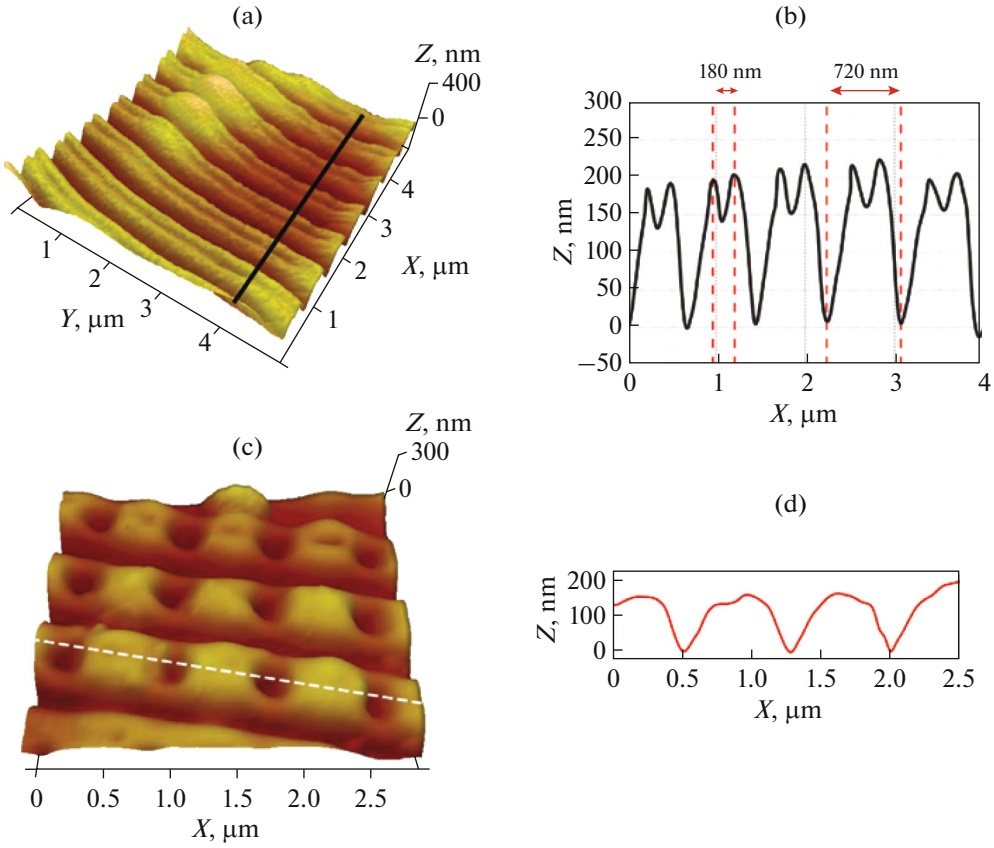

Fig. 7. Atomic force microscopy-based microphotographs (a, c) and profilograms (b, d) of the surface of an As_2S_3 film irradiated with 10 femtosecond laser pulses (100 fs, 800 nm) with energies of 0.1 (a, b) and 0.4 mJ (c, d) [92].

the accompanying ablation of the material from these regions.

A similar effect of ablation from the ridge of the As_2S_3 surface grating was observed in [92], but without changing the scanning strategy with femtosecond laser pulses (Figs. 7a and 7b).

The formation of nanocavities with an average diameter of 300 nm, periodically placed in the formed gratings, was also recorded (Figs. 7c and 7d). The formation of such nanocavities in ChVSs is presumably due to microexplosions and the relatively low thermal conductivity of As_2S_3, which causes increased heating of the material in certain areas corresponding to the maxima of the electromagnetic-field distribution during irradiation.

As a result, our analysis of all types of appearing hierarchical structures suggests that, during the formation of LIPSSs, it is sometimes necessary to take into account not only the model of plasmon-polariton excitation, but also the effects of local heating on nanoscales under the action of laser pulses.

Despite significant advances in the formation of LIPSSs in ChVSs such as GST225, As_2S_3, and As_2Se_3, it still cannot be said that the diversity of these structures is inherent in a wider range of ChVSs due to lack of works confirming this assumption to date. This is partly due to differences in the absorption spectra, thermal conductivity, and whole electronic subsystems in different ChVSs. Technologically, this means that the production of LIPSSs with the necessary quality for use in applications requires the selection of an individual set of parameters (wavelength, energy density, and number of structuring laser pulses), as well as scanning strategies and laser-beam focusing conditions, for each specific material. Nevertheless, the progress in the development of laser technology and related nanostructuring technologies gives hope for new results on the formation of LIPSSs for a wider range of ChVSs in the near future.

CONCLUSIONS

The above-presented review shows the possibility of transforming the local structure of ChVSs as a result of external optical, electrical, or thermal effects. These structural transformations can be reversible; they can be expressed both by the amorphous phase and by crystallization, which is described using mainly three approaches: the classical crystallization model, JMAK theory, and nonisothermal crystallization model.

In practice, effects of switching, memory, photodarkening, and photoinduced anisotropy can be observed as a result of the structural modification of ChVSs. The use of modern technologies for the microstructuring and nanostructuring of thin ChVS films makes it possible to create different types of metasurfaces and reconfigurable photonic elements, which can be used as optical modulators, polarization converters, diffractive optical elements, and IR light filters.

Of particular interest are structural transformations under the action of femtosecond laser pulses, when intense electronic excitation exceeds thermal processes in terms of the rate and efficiency of structural transformations. This makes it possible to carry out rapid structural transformations, in particular, data recording and rewriting. At the same time, it is possible to form surface gratings with wavelength and subwavelength periods based on the photoinduced generation of surface plasmon polaritons, which determine the periodic modulation of the relief and/or phase. Such structures have optical and electrophysical anisotropy, which is manifested in sensitivity to the polarization of incident radiation and the direction of the applied current, which makes it possible to significantly increase the density of information encoded by femtosecond-laser irradiation in phase-change ChVS films.

ACKNOWLEDGMENTS

We are grateful to L.A. Golovan, D.V. Shuleiko, A.V. Kolchin, P.I. Lazarenko, E.V. Kuzmin, P.A. Danilov, and S.I. Kudryashov for providing experimental and calculated data on thin ChVS films irradiated with femtosecond laser pulses.

FUNDING

The production of LIPSSs in thin arsenic-selenide films and analysis of the main patterns of the formation of such structures in ChVSs as a result of exposure to femtosecond laser pulses were supported by the Russian Science Foundation (grant no. 22-19-00035, https://rscf.ru/en/project/22-19-00035/).

CONFLICT OF INTEREST

The authors declare that they have no conflict of interests.

OPEN ACCESS

REFERENCES

1. M. Faraday, *Experimental Researches in Electricity. Series IV*, Philos. Trans. R. Soc. London **123**, 507–522 (1833).
2. W. Smith, Nature **7**, 303 (1873).
3. F. Braun, Ann. Phys. Chem. **153**, 556 (1874).
4. W. G. Adams and R. E. Day, Proc. R. Soc. A **25**, 113 (1876).
5. N. A. Goryunova and B. T. Kolomiets, Izv. Akad. Nauk SSSR, Ser. Fiz. **20**, 1496 (1956).
6. N. Mott, Science **201**, 871 (1978). https://www.doi.org/10.1126/science.201.4359.871
7. B. T. Kolomiets and E. A. Lebedev, Radiotekh. Elektron. **8**, 2097 (1963).
8. S. R. Ovshinsky, Phys. Rev. Lett. **21**, 1450 (1968). https://doi.org/10.1103/PhysRevLett.21.1450
9. https://www.extremetech.com/extreme/211087-intel-micron-reveal-xpoint-a-new-memory-architecture-that-claims-to-outclass-both-ddr4-and-nand
10. https://www.techinsights.com/blog/memoryselector-elements-intel-optanetm-xpoint-memory
11. https://www.techinsights.com/blog/intel-3d-xpoint-memory-die-removed-intel-optanetm-pcm-phase-change-memory
12. H. Zhang, C. X. Liu, X. L. Qi, et al., Nat. Phys. **5**, 438 (2009). https://doi.org/10.1038/nphys1270
13. W. Zhang, R. Yu, H. J. Zhang, et al., New J. Phys. **12**, 065013 (2010). https://doi.org/10.1088/1367-2630/12/6/065013
14. M. Koenig, S. Wiedmann, C. Brune, et al., Science **318**, 766 (2007). https://doi.org/10.1126/science.1148047
15. O. A. Pankratov, S. V. Pakhomov, and B. A. Volkov, Solid State Commun. **61**, 93 (1987). https://doi.org/10.1016/0038-1098(87)90934-3
16. A. V. Kolobov and J. Tominaga, *Two-Dimensional Transition-Metal Dichalcogenides* (Springer, Switzerland, 2016). https://www.doi.org/10.1007/978-3-319-31450-1
17. D. A. Bandurin, A. V. Tyurnina, G. L. Yu, et al., Nat. Nanotech. **12**, 223 (2017). https://doi.org/10.1038/nnano.2016.242
18. J. S. Berkes, S. W. Ing, Jr., and W. J. Hillegas, J. Appl. Phys. **42**, 4908 (1971). https://doi.org/10.1063/1.1659873
19. Y. Ikeda and K. Shimakawa, J. Non-Cryst. Solids **338–340**, 539 (2004). https://doi.org/10.1016/j.jnoncrysol.2004.03.037
20. K. Tanaka, Phys. Rev. B **57**, 5163 (1998). https://doi.org/10.1103/PhysRevB.57.5163

21. A. Kovalskiy, J. Cech, C. L. Tan, et al., Proc. SPIE **7273**, 1268 (2009). https://doi.org/10.1117/12.811646
22. S. I. Nesterov, M. E. Boyko, M. Krbal, and A. V. Kolobov, J. Non-Cryst. Solids **563**, 120816 (2021). https://doi.org/10.1016/j.jnoncrysol.2021.120816
23. K. Tanaka, Solid State Commun. **15**, 1521 (1974). https://doi.org/10.1016/0038-1098(74)90930-2
24. V. M. Lyubin and M. L. Klebanov, Semiconductors **32**, 817 (1998). https://doi.org/10.1134/1.1187513
25. A. Saliminia, T. V. Galstian, and A. Villeneuve, Phys. Rev. Lett. **85**, 4112 (2000). https://doi.org/10.1103/PhysRevLett.85.4112
26. A. V. Kolobov and S. R. Elliott, J. Non-Cryst. Solids **189**, 297 (1995). https://doi.org/10.1016/0022-3093(95)00245-6
27. S. A. Kozyukhin, P. I. Lazarenko, A. I. Popov, and I. L. Eremenko, Russ. Chem. Rev. **91**, RCR5033 (2022). https://doi.org/10.1070/RCR5033
28. X. Sun, M. Ehrhardt, A. Lotnyk, et al., Sci. Rep. **6**, 28246 (2016). https://doi.org/10.1038/srep28246
29. T. Kunkel, Yu. Vorobyov, M. Smayev, et al., J. Alloys Compd. **851**, 156924 (2021). https://doi.org/10.1016/j.jallcom.2020.156924
30. J. Siegel, W. Gawelda, D. Puerto, et al., J. Appl. Phys. **103**, 023516 (2008). https://doi.org/10.1063/1.2836788
31. M. Hada, W. Oba, M. Kuwahara, et al., Sci. Rep. **5**, 13530 (2015). https://doi.org/10.1038/srep13530
32. Y. H. Wang and F. R. Liu, J. Phys.: Conf. Ser. **1676**, 012161 (2020). https://doi.org/10.1088/1742-6596/1676/1/012161
33. M. E. Fedyanina, P. I. Lazarenko, Yu. V. Vorobyev, et al., Semiconductors **54**, 1775 (2020). https://doi.org/10.1134/S1063782620130060
34. N. A. Bogoslovskii and K. D. Tsendin, Semiconductors **46**, 559 (2012). https://doi.org/10.1134/S1063782612050065
35. C. R. de Galarreta, I. Sinev, A. M. Alexeev, et al., Optica **7**, 476 (2020). https://doi.org/10.1364/optica.384138
36. A. V. Pogrebnyakov, J. A. Bossard, J. P. Turpin, et al., Opt. Mater. Express **8**, 2264 (2018). https://doi.org/10.1364/OME.8.002264
37. W. Zhu, R. Yang, Y. Fan, et al., Nanoscale **10**, 12054 (2018). https://doi.org/10.1039/C8NR02587H
38. O. M. Efimov, L. B. Glebov, K. A. Richardson, et al., Opt. Mater. **17**, 379 (2001). https://doi.org/10.1016/S0925-3467(01)00062-3
39. V. I. Nalivaiko and M. A. Ponomareva, Opt. Spectr. **126**, 439 (2019). https://doi.org/10.1134/S0030400X19040179
40. G. Tammann and Q. A. Mansuri, Z. Anorg. Allg. Chem. **126**, 119 (1923).
41. G. Tammann, Z. Anorg. Allg. Chem. **157**, 321 (1926).
42. G. Tammann and R. F. Mehl, *The States of Aggregation* (**D**. Van Nostrand, New York, 1925).
43. W. A. Tiller, *The Science of Crystallization: Microscopic Interfacial Phenomena* (Cambridge Univ. Press, Cambridge, 1991). https://doi.org/10.1017/CBO9780511623158
44. *Crystallization: Basic Concepts and Industrial Application*, Ed. by W. Beckmann (Wiley-VCH, Weinheim, 2013).
45. A. Feltz, *Amorphe und Glasartige Anorganische Festkörper* (Akademie Verlag, Berlin, 1983). https://doi.org/10.1002/zfch.19850250223
46. S. A. Dembovskii and E. A. Chechetkina, *Glass Formation* (Nauka, Moscow, 1990) [in Russian].
47. A. N. Kolmogorov, Izv. Akad. Nauk SSSR, Ser. Mat. **1**, 355 (1937).
48. M. Avrami, J. Chem. Phys. **7**, 1103 (1939). https://doi.org/10.1063/1.1750380
49. W. A. Johnson and R. F. Mehl, Trans. AIME **135**, 416 (1939).
50. G. Ruitenberg, A. K. Petford-Long, and R. C. Doole, J. Appl. Phys. **92**, 3116 (2002). https://doi.org/10.1063/1.1503166
51. V. Weidenhof, I. Friedrich, S. Ziegler, and M. Wuttig, J. Appl. Phys. **89**, 3168 (2001). https://doi.org/10.1063/1.1351868
52. D. Claudio, J. Gonzalez-Hernandez, O. Lice, et al., J. Non Cryst. Solids **352**, 51 (2006). https://doi.org/10.1016/j.jnoncrysol.2005.11.007
53. M. Abu El-Oyoun, J. Non Cryst. Solids **357**, 1729 (2011). https://doi.org/10.1016/j.jnoncrysol.2011.01.038
54. J. Tominaga, T. Shima, P. Fons, et al., Jpn. J. Appl. Phys. **48**, 03A053 (2009). https:// www.doi.org/10.1143/JJAP.48.03A053
55. D. P. Birnie and M. C. Weinberg, Physica A (Amsterdam) **230**, 484 (1996). https://doi.org/10.1016/0378-4371(96)00124-0
56. M. C. Weinberg, Thermochim. Acta **280–281**, 63 (1996). https://doi.org/10.1016/0040-6031(95)02635-5
57. T. Kunkel, Yu. Vorobyov, M. Smayev, et al., Mater. Sci. Semicond. Process. **139**, 106350 (2022). https://doi.org/10.1016/j.mssp.2021.106350
58. I. V. Karpov, M. Mitra, D. Kau, et al., Appl. Phys. Lett. **92**, 173501 (2008). https://doi.org/10.1063/1.2917583
59. V. G. Karpov, Appl. Phys. Lett. **97**, 033505 (2010). https://doi.org/10.1063/1.3467458
60. M. Kadic, G. W. Milton, M. van Hecke, and M. Wegener, Nat. Rev. Phys. **1**, 198 (2019). https://doi.org/10.1038/s42254-018-0018-y
61. Z. Guo, H. Jiang, and H. Chen, J. Appl. Phys. **127**, 071101 (2020). https://doi.org/10.1063/1.5128679
62. N. S. Kumar, K. C. B. Naidu, P. Banerjee, et al., Crystals **11**, 518 (2021). https://doi.org/10.3390/cryst11050518
63. A. I. Solomonov, S. I. Pavlov, P. I. Lazarenko, et al., J. Phys.: Conf. Ser. **2103**, 012173 (2021). https://doi.org/10.1088/1742-6596/2103/1/012173

64. C. R. de Galarreta, A. M. Alexeev, Y.-Y. Au, et al., Adv. Funct. Mater. **28**, 1704993 (2018).
65. C.-Y. Hwang, G. H. Kim, J.-H. Yang, et al., Nanoscale **10**, 22635 (2018). https:// www.doi.org/10.1039/c8nr90254b
66. S. G.-C. Carrillo, L. Trimby, Y.-Y. Au, et al., Adv. Opt. Mater. **7**, 1801782 (2019). https://doi.org/10.1002/adom.201801782
67. M. N. Julian, C. Williams, S. Borg, et al., Optica **7**, 746 (2020). https://doi.org/10.1364/OPTICA.392878
68. S. Abdollahramezani, O. Hemmatyar, M. Taghinejad, et al., Nat. Commun. **13**, 1696 (2022). https://doi.org/10.1038/s41467-022-29374-6
69. M. Delaney, I. Zeimpekis, D. Lawson, et al., Adv. Funct. Mater. **30**, 2002447 (2020). https://doi.org/10.1002/adfm.202002447
70. S. Kozyukhin, M. Smayev, V. Sigaev, et al., Phys. Status Solidi B **257**, 1900617 (2020). https://doi.org/10.1002/pssb.201900617
71. S. Zabotnov, A. Kolchin, D. Shuleiko, et al., Micro **2**, 88 (2022). https://doi.org/10.3390/micro2010005
72. P. I. Trofimov, I. G. Bessonov, P. I. Lazarenko, et al., ACS Appl. Mater. Interfaces **13**, 32031 (2021). https://doi.org/10.1021/acsami.1c08468
73. X. Yu, D. Qi, H. Wang, et al., Opt. Express **27**, 10087 (2019). https://doi.org/10.1364/OE.27.010087
74. J. Bonse and S. Graf, Laser Photonics Rev. **14**, 2000215 (2020). https://doi.org/10.1002/lpor.202000215
75. J. E. Sipe, J. F. Young, J. Preston, and H. M. van Driel, Phys. Rev. B **27**, 1141 (1983). https://doi.org/10.1103/PhysRevB.27.1141
76. V. I. Emel'yanov, E. M. Zemskov, and V. N. Seminogov, Kvant. Elektron. **10**, 2389 (1983).
77. V. I. Emel'yanov, E. M. Zemskov, and V. N. Seminogov, Kvant. Elektron. **11**, 2283 (1984).
78. D. Shuleiko, M. Martyshov, D. Amasev, et al., Nanomaterials **11**, 42 (2021). https://doi.org/10.3390/nano11010042
79. S. S. Fedotov, A. G. Okhrimchuk, A. S. Lipatiev, et al., Opt. Lett. **43**, 851 (2018). https://doi.org/10.1364/OL.43.000851
80. A. S. Lipatiev, S. S. Fedotov, A. G. Okhrimchuk, et al., Appl. Opt. **57**, 978 (2018). https://doi.org/10.1364/AO.57.000978
81. R. Drevinskas, M. Beresna, M. Gecevičius, et al., Appl. Phys. Lett. **106**, 171106 (2015). https://doi.org/10.1063/1.4919538
82. M. Born and E. Wolf, *Principles of Optics* (Pergamon Press, 1959; Nauka, Moscow, 1973).
83. Y. Lei, M. Sakakura, L. Wang, et al., Optica **8**, 1365 (2021). https://doi.org/10.1364/OPTICA.433765
84. A. V. Kolchin, D. V. Shuleiko, S. V. Zabotnov, et al., J. Phys.: Conf. Ser. **1686**, 012006 (2020). https://doi.org/10.1088/1742-6596/1686/1/012006
85. S. Kozyukhin, P. Lazarenko, Yu. Vorobyov, et al., Opt. Laser Technol. **113**, 87 (2019). https://doi.org/10.1016/j.optlastec.2018.12.017
86. S. A. Yakovlev, A. V. Ankudinov, Yu. V. Vorob'ev, et al., Semiconductors, **52**, 809–815 (2018). https://doi.org/10.1134/S1063782618060246
87. A. Kolchin, D. Shuleiko, M. Martyshov, et al., Materials **15**, 3499 (2022). https://doi.org/10.3390/ma15103499
88. V. I. Ponomarenko and I. M. Lagunov, J. Commun. Technol. Electron. **66**, 403 (2021). https://doi.org/10.1134/S1064226921040094
89. D. Schmidt and M. Schubert, J. Appl. Phys. **114**, 083510 (2013). https://doi.org/10.1063/1.4819240
90. M. P. Smayev, P. I. Lazarenko, I. A. Budagovsky, et al., Opt. Laser Technol. **153**, 108212 (2022). https://doi.org/10.1016/j.optlastec.2022.108212
91. X. Yu, Q. Zhang, D. Qi, et al., Opt. Laser Technol. **124**, 105977 (2020). https://doi.org/10.1016/j.optlastec.2019.105977
92. S. H. Messaddeq, A. Dumont, A. Douaud, et al., Adv. Opt. Technol. **7**, 311 (2018). https://doi.org/10.1515/aot-2018-0031

Translated by D. Zabolotny